

Rothamsted Repository Download

A - Papers appearing in refereed journals

Gottselig, N., Amelung, W., Kirchner, J. W., Bol, R., Eugster, W., Granger, S. J., Hernández-Crespo, C., Herrmann, F., Keizer, J. J., Korkiakoski, M., Laudon, H., Lehner, I., Löfgren, S., Lohila, A., Macleod, C. J. A., Mölder, M., Müller, C., Nasta, P., Nischwitz, V., Paul-Limoges, E., Pierret, M. C., Pilegaard, K., Romano, N., Sebastià, M. T., Stähli, M., Voltz, M., Vereecken, H., Siemens, J. and Klumpp, E. 2017. Elemental Composition of Natural Nanoparticles and Fine Colloids in European Forest Stream Waters and Their Role as Phosphorus Carriers. *Global Biogeochemical Cycles*. 31 (10), pp. 1592-1607.

The publisher's version can be accessed at:

- <https://dx.doi.org/10.1002/2017GB005657>

The output can be accessed at: <https://repository.rothamsted.ac.uk/item/8v555>.

© 5 October 2017, Please contact library@rothamsted.ac.uk for copyright queries.



Global Biogeochemical Cycles

RESEARCH ARTICLE

10.1002/2017GB005657

Key Points:

- Stream phosphorus is largely bound to natural nanoparticles and colloids
- The chemical composition of colloids varies systematically from Northern to Southern European streams

Supporting Information:

- Supporting Information S1

Correspondence to:

E. Klumpp,
e.klumpp@fz-juelich.de

Citation:

Gottselig, N., Amelung, W., Kirchner, J. W., Bol, R., Eugster, W., Granger, S. J., ... Klumpp, E. (2017). Elemental composition of natural nanoparticles and fine colloids in European forest stream waters and their role as phosphorus carriers. *Global Biogeochemical Cycles*, 31, 1592–1607. <https://doi.org/10.1002/2017GB005657>

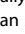
Received 23 FEB 2017

Accepted 29 SEP 2017

Accepted article online 5 OCT 2017

Published online 26 OCT 2017

Elemental Composition of Natural Nanoparticles and Fine Colloids in European Forest Stream Waters and Their Role as Phosphorus Carriers

N. Gottselig¹, W. Amelung^{1,2} , J. W. Kirchner^{3,4} , R. Bol¹, W. Eugster⁵ , S. J. Granger⁶, C. Hernández-Crespo⁷, F. Herrmann¹, J. J. Keizer⁸, M. Korkiakoski⁹ , H. Laudon¹⁰ , I. Lehner¹¹, S. Löfgren¹² , A. Lohila⁹ , C. J. A. Macleod¹³, M. Mölder¹⁴, C. Müller¹⁵ , P. Nasta¹⁶, V. Nischwitz¹⁷, E. Paul-Limoges⁵, M. C. Pierret¹⁸, K. Pilegaard¹⁹ , N. Romano¹⁶, M. T. Sebastià^{20,21}, M. Stähli²² , M. Voltz²³, H. Vereecken¹ , J. Siemens^{2,24}, and E. Klumpp¹ 

¹Institute of Bio- and Geosciences, Agrosphere (IBG-3), Jülich Research Center, Jülich, Germany, ²Institute of Crop Science and Resource Conservation – Soil Science and Soil Ecology, University of Bonn, Bonn, Germany, ³Department of Environmental Systems Science, ETH Zurich, Zurich, Switzerland, ⁴Swiss Federal Institute for Forest, Snow and Landscape Research (WSL), Davos, Switzerland, ⁵Institute of Agricultural Sciences, ETH Zurich, Zurich, Switzerland, ⁶Rothamsted Research, North Wyke, Devon, UK, ⁷Instituto de Ingeniería del Agua y Medio Ambiente, Universitat Politècnica de València, Valencia, Spain, ⁸Centre for Environmental and Marine Studies, Department Environment and Planning, University of Aveiro, Aveiro, Portugal, ⁹Atmospheric Composition Research, Finnish Meteorological Institute, Helsinki, Finland, ¹⁰Department of Forest Ecology and Management, Swedish University of Agricultural Sciences, Uppsala, Sweden, ¹¹Centre for Environmental and Climate Research, Lund University, Lund, Sweden, ¹²Department Aquatic Sciences and Assessment, Swedish University of Agricultural Sciences, Uppsala, Sweden, ¹³James Hutton Institute, Dundee, UK, ¹⁴Department of Physical Geography and Ecosystem Science, Lund University, Lund, Sweden, ¹⁵Department Catchment Hydrology, Stable Isotope Group, Helmholtz Center for Environmental Research, Leipzig, Germany, ¹⁶Department of Agricultural Sciences, Division of Agricultural, Forest and Biosystems Engineering, University of Napoli Federico II, Naples, Italy, ¹⁷Central Institute for Engineering, Electronics and Analytics, Analytics (ZEA-3), Jülich Research Center, Jülich, Germany, ¹⁸Laboratoire d'Hydrologie et Géochimie de Strasbourg, Ecole et Observatoire des Sciences de la Terre, Strasbourg, France, ¹⁹Department of Environmental Engineering, Technical University of Denmark, Kongens Lyngby, Denmark, ²⁰Laboratory of Functional Ecology and Global Change, Forest Sciences Centre of Catalonia, Catalonia, Spain, ²¹Group GAMES and Department of Horticulture, Botany and Gardening, School of Agrifood and Forestry Science and Engineering, University of Lleida, Lleida, Spain, ²²Mountain Hydrology and Mass Movements, Swiss Federal Institute for Forest, Snow and Landscape Research (WSL), Davos, Switzerland, ²³Institut National de la Recherche Agronomique, UMR LISAH, Montpellier, France, ²⁴Institute of Soil Science and Soil Conservation, Justus Liebig University Giessen, Giessen, Germany

Abstract Biogeochemical cycling of elements largely occurs in dissolved state, but many elements may also be bound to natural nanoparticles (NNP, 1–100 nm) and fine colloids (100–450 nm). We examined the hypothesis that the size and composition of stream water NNP and colloids vary systematically across Europe. To test this hypothesis, 96 stream water samples were simultaneously collected in 26 forested headwater catchments along two transects across Europe. Three size fractions (~1–20 nm, >20–60 nm, and >60 nm) of NNP and fine colloids were identified with Field Flow Fractionation coupled to inductively coupled plasma mass spectrometry and an organic carbon detector. The results showed that NNP and fine colloids constituted between $2 \pm 5\%$ (Si) and $53 \pm 21\%$ (Fe; mean \pm SD) of total element concentrations, indicating a substantial contribution of particles to element transport in these European streams, especially for P and Fe. The particulate contents of Fe, Al, and organic C were correlated to their total element concentrations, but those of particulate Si, Mn, P, and Ca were not. The fine colloidal fractions >60 nm were dominated by clay minerals across all sites. The resulting element patterns of NNP <60 nm changed from North to South Europe from Fe- to Ca-dominated particles, along with associated changes in acidity, forest type, and dominant lithology.

1. Introduction

Networks of small streams and large rivers transport mobile compounds over long distances and drive their export from the continents to the oceans (Bishop et al., 2008; Dynesius & Nilsson, 1994). Environmental water samples contain a wide variety of chemical species, including simply hydrated ions, molecules, colloidal particles, and coarser grains (Stumm & Morgan, 1981). The partitioning between these species controls

elemental cycling, transport, and loss processes (Stolpe et al., 2010). Understanding the distribution of the elements between different physicochemical binding forms is thus an important prerequisite for understanding the mechanisms of aquatic and terrestrial ecosystem nutrition (Benedetti et al., 1996; Hasseloev et al., 1999; Tipping & Hurley, 1992; Wells & Goldberg, 1991). This is especially important for those nutrients that are frequently limiting like phosphorus (P) (Jarvie et al., 2012). Indeed, the recent review by Bol et al. (2016) highlighted the (unexpected) scarcity of data on colloidal P fluxes in temperate forest ecosystems, which severely limits accurate quantification of forest P nutrition and losses.

Research on nutrient acquisition and cycling processes in stream waters and terrestrial ecosystems has often focused on the “dissolved fraction.” This fraction is frequently operationally defined as the aqueous phase that passes a $< 0.45 \mu\text{m}$ filter (Marschner & Kalbitz, 2003, and references therein). However, it is increasingly recognized that naturally occurring nanoparticles (NNP, $d = 1\text{--}100 \text{ nm}$), and also larger particles belonging to the overall term “colloids” ($d = 1 \text{ nm--}1 \mu\text{m}$), can be substantial components within this operational definition of elements present in the dissolved fraction. Colloids smaller than $0.45 \mu\text{m}$ ($\approx 450 \text{ nm}$) are in the present study defined as fine colloids. In natural aqueous phases up to 100% of the total elemental concentrations of metals, and also of specific nutrients like P, can be associated with such particles (Gottselig et al., 2014; Hart et al., 1993; Hill & Aplin, 2001; Jarvie et al., 2012; Martin, Dai, & Cauwet, 1995). Hence, identifying NNP and colloids in water samples is necessary to better understand the cycling and transport of elements in catchments and to determine their biological availability. Headwater catchments are specifically interesting for this analysis because their input variables can be closely defined, thereby facilitating data interpretation. However, it is unknown how the composition and size distributions of NNP and fine colloids vary between headwater catchments on a continental scale. Large-scale studies are advantageous in this context to identify more overarching and broadly applicable principles of NNP and fine colloid composition, and their variations, in natural waters.

Prior studies have performed pioneering investigations on particulate P pools in aqueous and terrestrial systems (e.g., Binkley et al., 2004; Espinosa et al., 1999; Sharpley et al., 1995), yet through the applicability of modern particle analysis/fractionation techniques, these functionally defined particulate fractions could be examined more closely and thus allow a more accurate subcategorization of elements in the “particulate” phase. Further, the focus of dissolved elements as being ions of (hydr)oxized elements in aqueous solution needs to be reconsidered due to the presence of particles within the operationally defined dissolved range (cf., e.g., Gimbert et al., 2003; Lyven et al., 2003; Regelink et al., 2011). In this regard, field flow fractionation (FFF; Giddings et al., 1976) is a viable tool for these analyses, because it is a nearly nondestructive technique for the fractionation of NNP and fine colloids, thus eliminating the need for pretreatments which can alter the particle composition or size range.

The specific reactivity of nanoparticles is high, in comparison to larger-sized colloids, (Hartland et al., 2013; Qafoku, 2010) rendering them potentially predominant carriers of nutrients in ecosystems. It has already been shown that NNP can bind the majority of P present in soil solutions (Hens & Merckx, 2001) and stream waters (Gottselig et al., 2014, 2017) and that they can even support plant uptake of P from solution (Montalvo et al., 2015). First results indicate that organic matter, Fe, and/or Al may be major binding partners for P in NNP of an acidic forest river system and that the binding of P varies depending on the stream water composition (Baken, Regelink et al., 2016; Gottselig et al., 2014). Under the acidic conditions that characterize many natural settings (particularly many coniferous forest soils), surfaces of metal (hydr)oxides are positively charged and thus act as strong binding partners for negatively charged nutrients like P (Hasseloev & von der Kammer, 2008; Richardson, 1985) and organic matter (Celi & Barberis, 2005). Adsorbed P and organic matter can even act as stabilizing agents for colloidal suspensions of particles (Ranville & Macalady, 1997; Six et al., 1999). Organic matter associated with NNP and larger colloids also contains P (Darch et al., 2014). Some authors even assume that in the smaller size ranges, organophosphorus compounds can also act as the primary building blocks of NNP (Regelink et al., 2013), although these building blocks are more commonly thought to be aluminosilicates, organic matter (org C) or oxides and/or hydroxides of iron (Fe), aluminum (Al), and manganese (Mn) (Baken, Regelink et al., 2016; Hartland et al., 2013; Lyven et al., 2003; Regelink et al., 2011). At elevated pH levels in stream water, calcium (Ca) is increasingly present in the colloids and associated with P in the form of Ca phosphates. These Ca phosphate colloids can either be in mineral form or associated on organic/organomineral complexes or clays. In the case of Ca colloids, Ca is enriched in the colloidal phase in comparison to larger suspended matter (Ran et al., 2000), especially when surface waters drain

Table 1
Characteristics of Each European Site

Site	Abbr.	MAT	MAP	Soil type	Dominant forest type	Bedrock type	Catch	Elev	Slope	Forest	MAR
Aneboda	AB	5.8	750	Podzol	Coniferous	Granite ^a	0.19	225	0.13	0.73	280
Agia	AG	15.8	691	Cambisol	Broadleaf	Gneiss ^b	0.75	916	0.28		
Allt a' Mharcaidh	AM	5.8	1110	Podzol	Coniferous	Granite ^a	9.79	716		0.02	
Bode	BO	7.1	1600	Cambisol	Coniferous	Shale and Greywacke ^a	1.27	515	0.07	1.00	
Barranco de Porta Coeli	BPC	14.5	450	Fluvisol	Mixed	sandstone ^a	3.20	523	0.21	0.50	
Costiglione	CO	15.9	1183	Cambisol	Broadleaf	Carbonatic ^b	11	563	0.32	1.00	225
Cotley Wood	CW	10.1	1044	Cambisol	Broadleaf	Siltstone	0.50	146	0.08	1.00	
Erlenbach	EB	6.0	2294	Gleysol	Coniferous	Flysch	0.73	1330	0.24	0.39	1778
Franceschiello	FR	15.9	1183	Cambisol	Broadleaf	Carbonatic ^b	11	563	0.32	1.00	225
Gårdsjön	GS	6.7	1000	Podzol	Coniferous	Granite ^a	0.07	127	0.22	0.65	520
Krycklan	KR	1.8	614	Podzol	Coniferous	Greywacke ^a	679	260		0.87	311
Lettosuo	LE	4.6	627	Histosol	Coniferous	Gneiss	1.25	111	0.01	1.00	413
Lägeren	LÄ	8.4	930	Cambisol	Broadleaf	Limestone ^b		680	0.35	1.00	
Montseny	MS	9.0	870	Inceptisol	Coniferous	Schist					
La Peyne	LP	12.0	818	Leptosols	Broadleaf	Schist ^a	110	305	0.25	1.00	
Lümpenbach	LÜ	6.0	2426	Gleysol	Coniferous	Flysch	0.88	1260	0.15	0.19	2001
Lourizela	LZ	13.8	1300	Cambisol	Coniferous	Schist ^a	0.65	365	0.37	1.00	775
Norunda	NO	5.5	730	Regosol	Coniferous	Granite ^a	6084	45		1.00	250
Pallas	PA	-1.4	484	Podzol	Coniferous	Granite ^a	5.15	308	0.08	0.60	220
Piano Rabelli	PR	15.9	1183	Cambisol	Broadleaf	Carbonatic ^b	11	563	0.32	1.00	225
Ribera Salada	RS	15.6	800	Cambisol	Broadleaf	Carbonatic ^b		1483		1.00	
Soroe	SR	8.5	564	Mollisol	Broadleaf	(Glacial moraine) ^b		37	0.07	1.00	
Strengbach	SB	6.0	1400	Podzol	Coniferous	Granite ^a	0.80	1015	0.15	1.00	814
Serra de Cima	SC	13.8	1300	Cambisol	Broadleaf	Schist ^a	0.52	432	0.16	1.00	775
Vogelbach	VB	6.0	2159	Gleysol	Coniferous	Flysch	1.58	1285	0.23	0.63	1601
Wüstebach	WB	7.0	1220	Cambisol	Coniferous	Shales ^a	3.85	612	0.04	1.00	280

Note. Climate data, bedrock and soil type, and dominant forest type provided by site operators. Abbr. = abbreviation, MAT = mean annual temperature (°C), MAP = mean annual precipitation (mm), catch = catchment size (km²), elev = average elevation (m), slope = average slope, forest = proportion forest cover, MAR = mean annual runoff (mm).

^aSiliceous bedrock group. ^bCarlicareous bedrock group (see later Table 4).

carbonate-rich soils (Hill & Aplin, 2001). This highlights that Ca may also be a building block element of colloids (Dahlqvist et al., 2004), depending on stream water chemistry. The pH-dependent speciation of elements and their related affinity to particles give rise to the hypothesis examined in our study, which states that the composition and size distribution of NNP and fine colloids may not be uniform across large regions. If this is not the case, at least the speciation of elements and their presence in particle fractions would be expected to differ between acidic and alkaline stream waters.

Despite their important role in element binding, NNP and fine colloids were not considered as a substantial contributor to nutrient cycling in the past (e.g., Vitousek, 1982) and are still often neglected in pioneering studies on the analysis of influential factors on terrestrial nutrient availability (e.g., Fernández-Martínez et al., 2014). Examining the significance of NNP and fine colloids as well as their composition as a function of forest stream water pH on a continental scale can provide insights into their ecological relevance, particularly if one can use basic water quality parameters to estimate the total elemental concentrations that are associated with NNP and colloids. Better information on the chemical form and reactivity of elements in the putative “dissolved” fraction, in turn, can improve estimates of nutrient availability to plants and microorganisms.

For this study, it was hypothesized that NNP and fine colloids are ubiquitous carriers for elements in forested European river systems but that their composition varies along continental-scale gradients. The respective variations in climate, vegetation, soil, and freshwater characteristics (e.g., pH) substantially influence the physicochemical forms of P and other ecologically important constituents in forested freshwaters, thus, potentially revealing systematic controlling effects on NNP and fine colloid concentrations and composition. To test this hypothesis, 96 stream water samples from 26 forested sites from across Europe were collected. These 26 sites cover a wide range of soil types and parent materials, under deciduous or coniferous forests, over very differently sized catchments, and spanning different elevations and topographic gradients

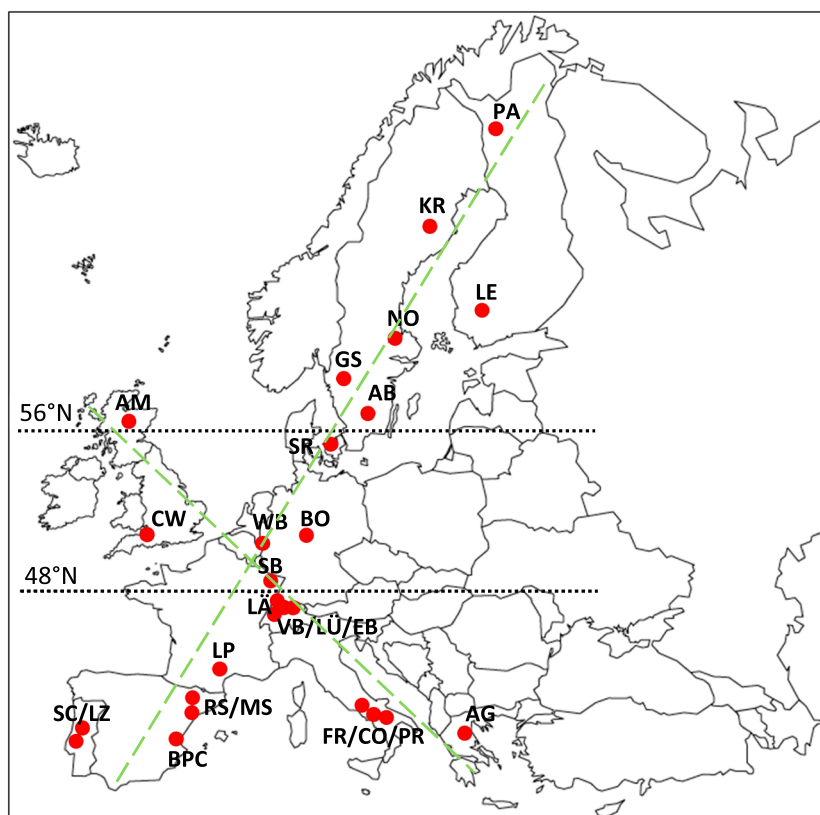


Figure 1. Location of the 26 sampling sites in Europe along two transects (green dashed lines). Site abbreviations are as follows: Pallas (PA) and Lettosuo (LE), Finland; Krycklan (KR), Norunda (NO), Gårdsjön (GS) and Aneboda (AB), Sweden; Soroe (SR), Denmark; Allt a' Mharcaidh (AM) and Cotley Wood (CW), United Kingdom; Wüstebach (WB) and Bode (BO), Germany; Lägeren (LÄ), Vogelbach (VB), Lümpenbach (LÜ) and Erlenbach (EB), Switzerland; Franchesiello (FR), Costigliano (CO) and Piano Rabelli (PR), Italy; Agia (AG), Greece; Strengbach (SB) and La Peyne (LP), France; Ribera Salada (RS), Montseny (MS) and Baranco de Porta Coeli (BPC), Spain; Sierra de Cima (SC) and Lourizela (LZ), Portugal. Black dotted lines indicate geographical separation between northern (north of 56°N), middle (between 48°N and 56°N) and southern (south of 48°N) sites.

(Table 1). FFF (Giddings et al., 1976; Hasseløev et al., 1999; Regelink et al., 2014), coupled online to high-precision elemental detectors, was used for the fractionation of NNP and colloids. To untangle the importance of single factors, a correlation matrix between all particulate elemental concentrations, total elemental concentrations, and the basic site parameters such as mean annual temperature (MAT), mean annual precipitation (MAP), forest coverage, slope inclination, and runoff was also investigated.

2. Materials and Methods

2.1. Sampling

Twenty-six sites throughout Europe were selected along two transects, one from northern Finland to Portugal and the other from Scotland to Greece (Figure 1 and Table 1). Each site is a forested headwater catchment with low-intensity forest management practices, high tree coverage, and without inflows from urban or agricultural settings (for site abbreviations, see Table 1). Mean annual temperatures ranged between -1.4°C (PA, Finland) and $+15.9^{\circ}\text{C}$ (FR, CO, and PR, Italy) and mean annual precipitation ranged between 450 mm (BPC, Spain) and 2426 mm (LÜ, Switzerland) (Table 1). It was possible to assign a clear dominant forest type for 25 of the 26 sites (either coniferous or broadleaf), while the BPC site had 50% coniferous and 50% broadleaf tree species. Additionally, data on catchment size, average elevation, average slope, percentage forest cover, and mean annual runoff were collected where available (Table 1). All data were provided by the current site operators. During sampling, the electrical conductivity, pH, and water temperature of the water samples ranged substantially from $13\ \mu\text{S}/\text{cm}$ (SB) to $1775\ \mu\text{S}/\text{cm}$ (BPC), from 4.2 (GS) to 9.5 (RS), and

from 1.0°C (PA) to 19.9°C (RS) (for complete data of all main stream and tributary samples, see supporting information Table S1). Up to six samples were taken per site in May 2015 in order to derive a snapshot of NNP and fine colloid composition and their relevance for P transport across Europe at a given time of the year. The sampling locations were defined in consultation with the site operators to best reflect main and tributary streams of each catchment, similar to the approach of Gottselig et al. (2014). Sampling was conducted during base flow conditions. The sampling resulted in a total of 96 samples taken in duplicates in precleaned PE and glass bottles and shipped cooled to the lab; analysis of NNP and fine colloids was completed within 1 week after sampling. Own unpublished data indicate that during 1 week there is no significant alteration in the size distribution of NNP and fine colloids, despite selected risks of minor particle reaggregation in the larger size range. To minimize the risk of systematic errors due to sampling storage and pretreatment, all samples were handled, treated, and analyzed in equal manner.

2.2. Asymmetric Flow Field Flow Fractionation

Fractionation of the particles was performed with Asymmetric Flow Field Flow Fractionation (AF⁴). Briefly, a 0.5 mm spacer, a 1 kDa polyether sulfone membrane, and a 25 μM NaCl eluent solution were applied. About 5 mL of the PE bottled samples was injected into the AF⁴ system at 0.3 mL/min tip flow and 3 mL/min cross flow and focused for 30 min with 3.2 mL/min focus flow. Thereafter, a 30 min linear cross-flow gradient down to 0 mL/min with subsequent 40 min constant elution at a detector flow of 0.5 mL/min was applied. Reference materials (Suwanee River NOM, Humic Acid Standard II, and Fulvic Acid Standard II, International Humic Substances Society, Denver, USA; Sulfate Latex Standards 8% w/v 21–630 nm; Postnova Analytics, Landsberg, Germany) were used with the same AF⁴ conditions used for the samples for calibration of the particle diameters included in each size fraction. No reference material exists that covers the diverse particle morphologies and elemental concentrations of environmental samples. Therefore, the specified hydrodynamic diameters of the particles are equivalent sizes based on the elution time of the reference materials (c.f. Neubauer et al., 2011; Regelink et al., 2013; Stolpe et al., 2010). The lower size range of the first fraction was estimated according to the molecular weight cutoff (MWCO) of the membrane.

Online coupling of a UV detector (254 nm) served to initially determine peak elution and turbidity of the particle fractions. A dynamic light scattering (DLS) device was coupled for online size measurements of the largest size fraction. Blank runs inserted between sample runs in the measurement sequence showed no pronounced peaks. A quadrupole inductively coupled plasma–mass spectrometer (ICP-MS) with helium collision cell technology (Agilent 7500, Agilent Technologies, Japan) and for size-resolved detection of organic carbon an Organic Carbon Detector (OCD; DOC Labor, Karlsruhe, Germany) was coupled online to the AF⁴. The ICP-MS allowed size-resolved detection of Al, Si, P, Ca, Mn, and Fe, and the OCD allowed size-resolved detection of organic carbon. The ICP-MS system was calibrated through a postcolumn (Nischwitz & Goenaga-Infante, 2012) multipoint linear calibration injected via a T junction between the AF⁴ and the ICP-MS at 0.5 mL/min AF⁴ injection flow (= detector flow; no cross flow). The standard solutions (0 μg/L, 25 μg/L, 100 μg/L, 250 μg/L, and 500 μg/L) and the internal standards Rh and Y were dissolved in 0.5 mol/L HCl. This calibration technique is more complex than injecting the calibration standards directly into the AF⁴ system, but allows more precise correction of instrumental drift and calibration to higher concentrations without potentially contaminating the following sample (because the standards do not pass through the AF⁴). The variations of the ICP-MS peak areas for triplicate measurements of a representative sample were calculated to be 5.9% for P, 7.6% for Al, 14.0% for Si, 5.3% for Mn, and 15.6% for Fe. The limit of detection was 0.1 μg/L for P, 0.01 μg/L for Al, 3.3 μg/L for Si, 0.01 μg/L for Mn, and 0.02 μg/L for Fe. Quantitative atomization of the particles in the plasma has already been shown by Schmitt et al. (2002).

For the OCD coupling, 1 mL sample volume from the glass bottles was injected and focused for 10 min; the remaining parameters were the same as for ICP-MS coupling. The OCD system was calibrated using dilutions of Certipur® liquid TOC standard (EN 1484-H3/DIN 38409-H3, potassium hydrogen phthalate in water, stabilized, 1,000 mg/L; Merck Millipore 109017) in double-distilled water at concentrations of 0.05 mg/L, 0.1 mg/L, 0.5 mg/L, 1.0 mg/L, 3.0 mg/L, and 5.0 mg/L. The same calibration standards were also used in determining the total organic carbon in the stream water samples. For this determination, the AF⁴ channel was bypassed by connecting the tip inflow tubing to the detector outlet tubing of the channel. The runtime of the AF⁴ method for this data acquisition was 20 min at 0.5 mL/min tip flow. The relative standard deviation of the organic

carbon concentration for triplicate measurements of a representative sample was calculated to be 2.2%. The limit of detection for organic C was 0.01 mg/L.

2.3. Quality Control

First investigations on the stability of NNP and colloids were conducted prior to the sampling campaign to elucidate which sampling, storage, and transport procedures best reflect natural conditions at the time of measurement. This resulted in a sampling of unprocessed stream water with polypropylene containers; only samples for organic carbon analysis were taken with precleaned and preequilibrated glass vials. Samples were always taken in order moving upstream, from the catchment outlet to the headwaters. Containers were preconditioned in triplicates with stream water before the sample was taken from the center of the flowing stream without disturbing the sediment. Larger-sized particulates (e.g., visible parts of leaves) were not included in the water sample. For transport and storage, the samples were kept at a cool to ambient temperature, but neither were they frozen nor did their temperature ever exceed the stream temperature at sampling. Sample analysis was conducted as soon as possible after sampling, especially for organic carbon analysis. The analyses were performed in the order the samples arrived. For a more detailed discussion of circumstances affecting colloidal stability, see Buffle and Leppard (1995).

Immediately prior to analysis, samples were homogenized through agitation then filtered through 5 μm cellulose nitrate filters (GE Healthcare, Munich, Germany) to avoid clogging of the micrometer-sized AF⁴ tubing. No interference of cellulose and/or cellulose nitrate compounds with the org C signal was expected because both are insoluble in water (Hagedorn, 2006; Roth, 2011). Still, the filters were prerinsed with 15 mL double-deionized water to eliminate eventual bleeding compounds. Caking was prevented by filtering only small sample volumes up to 15 mL. Additionally, more than one filter was available per sample, but this was not needed due to the low turbidity of the samples. Filtration at 0.45 μm was purposely not performed, to avoid the risk of excluding particles not specific to the given size due to unknown morphological heterogeneity of the natural particles. Avoiding filtration also avoided the risk of membrane clogging when filtering occurs close to target size ranges of the analytes, which can result in a severe risk of underestimating NNP and fine colloidal concentrations (Zirkler et al., 2012).

The recovery of NNP and fine colloids fractionated by AF⁴ is greatly influenced by interactions of the natural particles with the membrane, particularly during focus time and at long and/or high cross flows. For natural samples, a portion of the sample was thus withdrawn from the fractionation process and measured by independent ICP-MS analysis (cf. section 3.1), thereby allowing us to relate element yields after fractionation to those without AF⁴ treatment. This analysis showed that the different elements associated to NNP and fine colloids ranged up to 99.5% of total elemental concentration, showing that generally there was no major particle loss. A more in-depth investigation of the AF⁴ recoveries with synthetic iron oxyhydroxide colloids revealed recoveries between 70 and 93% (Baken, Moens et al., 2016). These results are encouraging also for natural samples due to the similarity of the particle constituents.

2.4. Analysis of Raw Data

ICP-MS raw data were collected in counts per second (cps) using the MassHunter Workstation Software (Agilent Technologies, Japan), and OCD raw data were recorded in volts detector signal (V) with the AF⁴ analytical software (Postnova Analytics, Landsberg, Germany). Raw data were exported to Excel® (Microsoft Corporation, Redmond, USA) for baseline correction, peak integration, and conversion of peak areas to concentrations through multipoint linear calibration. Different pools of elements were considered in this study: (a) elemental concentrations assigned to the first, second, or third size fraction of NNP and fine colloids (see section 3.1 for explanation), (b) all particulate elemental concentrations, reflecting the sum of (e.g.) Fe concentrations in the first, second, and third fractions combined, and (c) the total concentration of an element in the sample prior to fractionation. The collective term colloids is occasionally used in our study as an encompassing term for the whole size range of nanoparticles and colloids. Concentrations are primarily given in $\mu\text{mol/L}$ for Al, Si, P, Ca, Mn, and Fe and in mmol/L for org C.

Stream water pH at sampling time was classified according to the Soil Survey Division of the Natural Resources Conservation Service, U.S. Department of Agriculture (U.S. Department of Agriculture, 1993), in order to clarify the influence of stream water pH and associated covariates on the relationships between NNP and fine colloid concentrations and total concentrations. According to this classification, acidic is

defined as $\text{pH} < 6.6$, neutral pH between 6.6 and 7.3, and alkaline pH values > 7.3 . Thus, pH was transformed into a semiquantitative variable, where each range of values is assigned to a given category.

Predictability of elemental concentrations through total concentrations was assessed through \log_{10} transformation of the elemental concentrations in the fractions and the total sample concentrations. Here we only considered regressions that achieved an $r \geq 0.71$. Further, sites were classified according to location (north, middle, and south) in Europe. To test if this zoning was able to differentiate element distributions of the NNP and other fine colloidal fractions, we focused on particulate Fe as redox-sensitive element and particulate Si as an indicator of siliceous bedrock and clay minerals. Also, we classified the study sites by major soil types (dystrophic, eutrophic, and semiterrestrial) and bedrock lithologies (siliceous, calcareous, and flysch), as well as two main forest types (coniferous/needle versus broadleaf versus mixed; see Table 1). Dystrophic soils included Podzols, as well as coniferous Cambisols, Leptosols, and Regosols; eutrophic soils were deciduous Cambisols, Leptosols, and Mollisols; semiterrestrial soils were Fluvisols and Gleysols (the sole Histosol was not included in this group comparison). Siliceous bedrock included all bedrock types except calcareous stone, limestone, and flysch. Flysch was assigned to a specific bedrock group, because it usually contains both carbonates and silicate minerals; the respective soils sampled were Gleysols (Table 1).

Further, the dependency of elements in the NNP and fine colloid fractions on the total elemental concentration and the potential predictability of NNP and fine colloidal composition were analyzed through correlation analysis with Pearson r coefficients, pairwise deletion of missing data (JMP 12.2.0, SAS Institute Inc., USA), and significance testing using nonparametric group comparisons with the Mann-Whitney U test for comparisons between two sample sets and with the Kruskal-Wallis analysis of variance (ANOVA) for comparisons among more than two sample sets (Statistica, Version 13, Dell Inc., Tulsa, USA). To facilitate the examination of controlling factors of NNP and fine colloid composition, correlation matrices followed by principal component analysis (Statistica, Version 13, Dell Inc., Tulsa, USA) served as an additional tool to reduce the number of variables and reveal a first structure in the relationships between the variables. Through this, we aimed at an identification of the site parameters, which are influential on particulate elemental concentrations. Varimax raw was applied as the rotational strategy for the analysis, to maximize the variances of the squared raw factor loadings across variables for each factor. Here casewise deletion of missing data was undertaken to ensure that the same number of cases entered into every analysis. Initially, calculations of the Kaiser-Meyer-Olkin Measure of Sampling Adequacy (KMO value; IBM SPSS Statistics 22) were performed to extract site parameters suitable for PCA analysis. When using all data, KMO was 0.5 and the PCA result was not stable against random elimination of input data; only with selected input variables, a $\text{KMO} > 0.6$ was achieved and the PCA was stable against variations in input data. As a follow-up tool, stepwise multiple regression was used, but it did not yield meaningful results due to the remaining complex interplay of the data.

3. Results and Discussion

3.1. Fractionation of Nanoparticles and Fine Colloids

Similar to findings for a forested watershed in Germany (Gottselig et al., 2014), the application of the AF^4 technique to other forested sites across Europe revealed distinct fractions of nanoparticles and fine colloids depending on the element investigated (Figures 2a and 2b; cf. supporting information Table S2). In total, three fractions of NNP and/or fine colloids were distinguishable for most (out of 96 samples, in 58.3% org C and Si were found in all three fractions, in $> 85\%$ for Ca and P, and in $> 95\%$ for Al, Mn, and Fe; cf. supporting information Table S2) samples. The fractograms included a peak of small-sized nanoparticles (first fraction), a second peak consisting of intermediate-sized nanoparticles (second fraction), and a third peak containing the largest-sized nanoparticles and fine colloidal matter (see also peak separation by dashed lines on the x axis in Figure 2). The peak pattern for each sample is represented by the fractograms of each element (see Figure 2). The second peak as shown for Krycklan, Sweden, was mainly defined through the Ca signal (violet; Figures 2a and 2b) due to the absence of other elemental peaks in the second fraction. P was variably detected in one, two, or three size fractions (Figures 2c and 2d; cf. supporting information Table S2). Hence, three different size fractions were isolated in this work, in close agreement with Stolpe et al. (2010), who also found three to four fractions of NNP and fine colloids in the lower Mississippi River, the largest river in North America.

Nanoparticles were the exclusive constituent of the first two fractions and, based on hydrodynamic diameters, accounted for approximately 20% in the third fraction. The first and second fractions consisted of

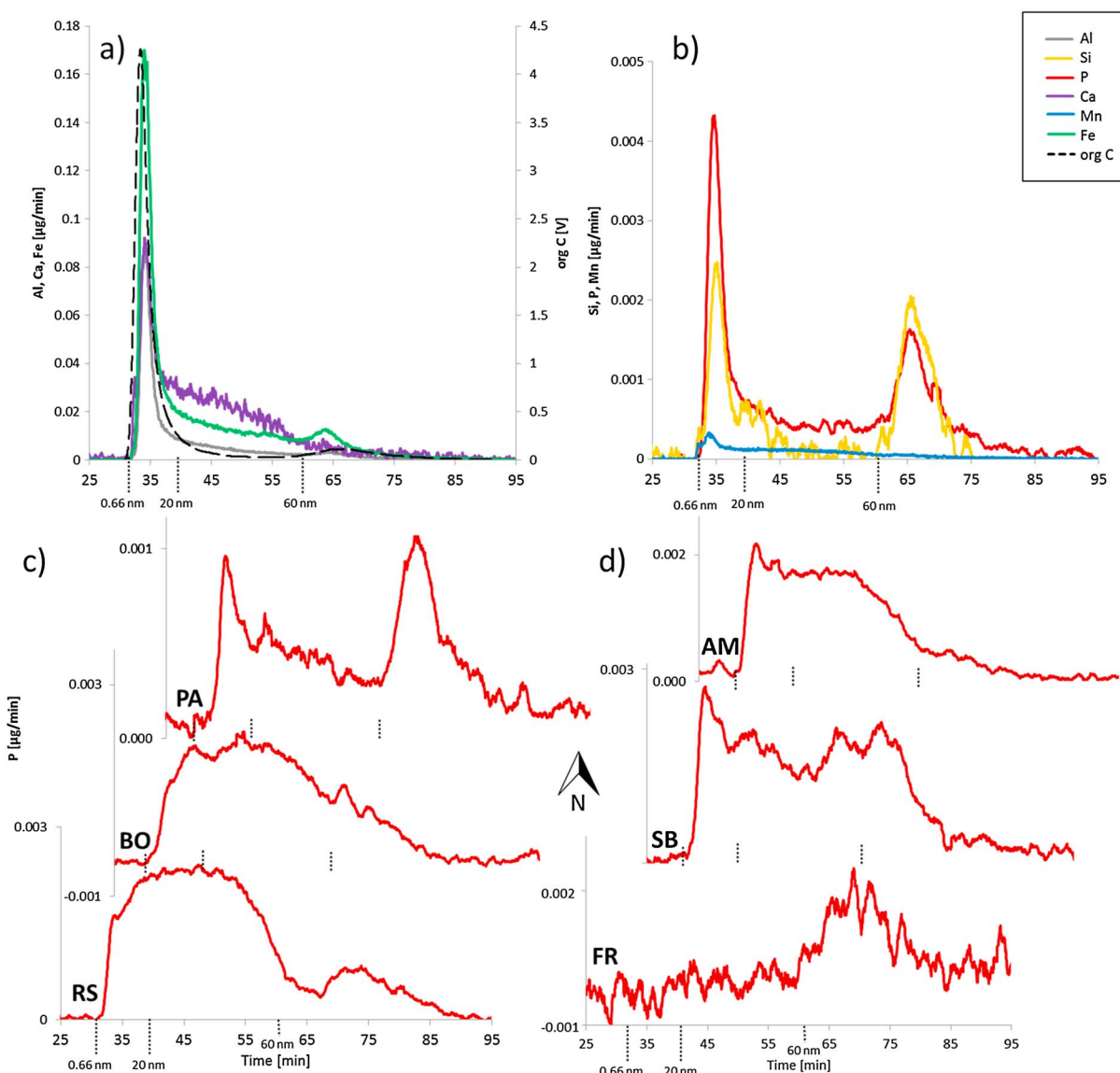


Figure 2. AF⁴-ICP-MS and AF⁴-OCD raw data fractograms. (a) Fractogram of Al, Ca, Fe, and org C of one sampling point at Krycklan, Sweden. (b) Fractogram of P, Si and Mn of same sampling point as a) at Krycklan, Sweden. (c) Fractogram of P of three sampling points at sites in South, Middle, and North Europe (increasing °N, y axis), North: PA = Pallas, Finland, Middle: BO = Bode, Germany, South: RS = Ribera Salada, Spain. (d) Fractogram of P of three sampling points at sites in South, Middle, and North Europe (increasing °N, y axis), North: AM = Allt a'Mharcaidh, Scotland, Middle: SB = Strengbach, France, South: FR = Franchesiello, Italy. X axes represent the method time in minutes. Focus time was partially cut off. Y axes for Al, Si, P, Ca, Mn, and Fe reflect mass flow in µg/min and for org C detector signal in V. Fraction borders apply to the ICP-MS signal; for the OCD evaluation these borders were modified because OCD peaks exhibit peak broadening due to the high volume of the OCD reactor.

nanoparticles with standard equivalent hydrodynamic diameters ranging from 1 kDa (equivalent to 0.66 nm, equation 2.2, Erickson, 2009) to 20 nm and from above 20 nm to 60 nm, respectively. The third fraction included nanoparticles larger than 60 nm up to fine colloids of approximately 300 nm in diameter. The DLS measurements revealed this maximum particle size for all measured samples (c.f. Gottselig et al., 2014, 2017). Hence, all detected NNP and fine colloids fell into the operationally defined “dissolved phase” (< 0.45 µm). Substantial signals of the elements Fe, P, Mn, Al, C, and Si were recorded in all three size fractions with varying intensities, confirming widespread occurrence of NNP and fine colloids in the size range < 450 nm.

The fractograms for P are markedly different among three sites spanning across one transect in Europe (Pallas in North Europe, Bode in Middle Europe, and Ribera Salada in South Europe; PA, BO, and RS in Figure 2c), consistent with the hypothesis that NNP and fine colloid composition and size distribution vary across the

continental scale. More generally, we observed differences in the P distribution within NNP and fine colloids among the various forested headwater catchments in Europe, that is, sometimes the particulate P was associated with clearly distinct fractions (e.g., PA; Figure 2c), whereas for other samples a less distinct fractionation of P (e.g., BO; Figure 2c) was observed. This exemplary described variation of elemental concentrations in the three fractions was observed for all recorded elements, supporting the general hypothesis that there are differences in the elemental composition between fractions and among the selected European streams. These patterns were found to be related to site-specific properties such as climate, water chemistry, soil type, and total stream water elemental concentrations, that is, we tested in the following to systematize the differences according to element composition and site properties.

3.2. Significance of NNP and Fine Colloids for Element Partitioning in Water Samples

The percentages of elements bound to NNP and fine colloids (i.e., percentage of all particulate elemental to total elemental concentration) demonstrated the substantial contribution of NNP and fine colloids to element fluxes in natural waters. The average percentages of elements found in the NNP and colloid phases were 53% for Fe (within the bounds for an interquartile range of 42–65%), 50% for P (36–70%), 26% for Mn (4–47%), 41%, for Al (28–56%), and 20% for organic C (5–28%) but only 2% for Si (0.1–0.4%) and 4% for Ca (0–5%; $n = 96$). The respective median values were 55% (Fe), 51% (P), 10% (Mn), 37% (Al), 11% (org C), 0.2% (Si), and 1% (Ca). Further, up to 99% of Fe, 96% of P and Mn, 95% of Al, 92% of org C, 46% of Si, and 27% of Ca were found associated with NNP and fine colloids, relative to the bulk elemental concentrations measured offline in the untreated samples. Overall, the percentages reflected a substantial contribution of the NNP and fine colloidal fractions within the operationally defined dissolved elements Fe, P, Al, org C, and Mn (in descending order). Previous research on the significance of colloid-bound elements within the operationally defined dissolved fraction also indicated maximum Fe binding in fine colloidal form between 80 and 100% with averages between 50 and 90% (Hill & Aplin, 2001; Jarvie et al., 2012; Martin et al., 1995), for organic C between 40 and 80% with averages between 20 and 60% (Jarvie et al., 2012; Martin et al., 1995; Wen et al., 1999), and for Al around 40 to 50% with averages around 45 to 55% (Hill & Aplin, 2001; Jarvie et al., 2012). Hill and Aplin (2001) determined that the fine colloidal fraction accounted for up to 50% of Mn (average 23%) and up to 30% of Ca (average 20%) but only up to 10% of Si (average 0%). Dahlqvist et al. (2004) found an average of 16% fine colloidal Ca in an Arctic river and in Amazonian rivers (also assessed with FFF). Data on total P are scarce, but Jarvie et al. (2012) reported that a fraction of up to 90% (averaging 66%) of organophosphorus compounds was associated with fine colloids in mixed land use sites, and Missong et al. (2016) and Jiang et al. (2015) also detected organophosphorus in the NNP and fine colloid fractions in soil samples. In summary, the present data indicate that the particulate form of elements is substantial in streams and that there are varying contributions of NNP and fine colloids to overall element fluxes across Europe.

3.3. Predictability of NNP and Fine Colloid Elemental Composition

The discrepancy between NNP and fine colloid and total elemental concentrations is potentially due to dissolved species in size ranges below the membrane MWCO when excluding the presence of larger particles. Two types of relationships between NNP and fine colloid concentrations and total concentrations could be observed, independent of the fraction in question. For Si, P, Ca, and Mn, we found scattered relationships between total concentrations and NNP/fine colloid concentrations (Figure 3, top left and bottom left). The concentrations of these elements that were bound to NNP and fine colloids did not change systematically with total elemental concentrations. All three size fractions of these elements showed such scattered relationships, although their median concentration varied (Table 2). By contrast, for Fe, Al, and org C, we found positive log-log relationships between total concentrations and colloidal concentrations (Figure 3, top right and bottom right).

The regression slopes of the log-log relationships between the particulate and total element concentrations differed among the three size fractions of Fe, Al, and org C (Table 2), which could reflect differences in Fe, Al, and org C speciation as stream water variables change but could also be related to site differences in the surface properties of mineral binding partners (which were not investigated here). Most interestingly, the log-log slope of the first size fraction Fe was 1.0 (Table 2 and Figure 3, top right and bottom right). This implied that across all European sites, on average, a constant proportion of total Fe was present in this very fine nanoparticulate fraction (<20 nm) and thus was independent of their stream water pH. This proportion was estimated to be 15%. Slopes for Fe in the second and third fractions, as well as for Al and org C for of all three

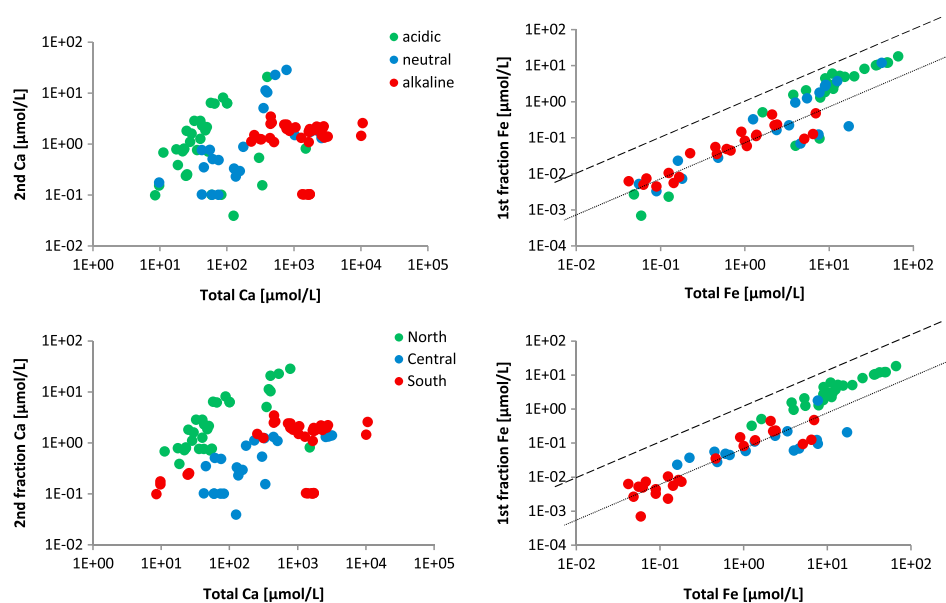


Figure 3. Examples for the two relations of particle concentration as function of the total element concentrations. (top left) Scatter diagram of \log_{10} -transformed data of second fraction Ca, as an example of the behavior of Si, P, Ca, and Mn across all fractions. (top right) Linear distribution of \log_{10} -transformed data for first fraction Fe, as an example of the behavior of Fe, Al, and org C across all fractions; color coding represents pH class of the site (cf. Table S1); acidic pH <6.6, neutral pH 6.6–7.3, alkaline pH >7.3. (bottom left and right) Same data as Figure 3 top left and top right but with color coding according to geographic regions (cf. Figure 1). Second fraction Ca was chosen opposed to first fraction Ca for the left diagram because the second fraction often exhibited a Ca peak (cf. Figure 2a). Dashed line represents 1:1 line and dotted line average proportion of total Fe present in the first fraction. $n = 96$.

fractions, were not parallel to the 1:1 line (not shown), instead indicating power law relationships (rather than a fixed NNP or fine colloid fraction). In contrast, for the elements that did not change systematically with total elemental concentrations (Ca, Si, Mn, and P) the median varied among the different size fractions as well as the percentage of particulate elemental concentration present in the fractions (cf. Table 2). The reasons for the different regression slopes and medians are still unclear and warrant investigation in future studies, potentially in combination with measurements of discharge-dependent concentration variations as shown in, for example, Trostle et al. (2016).

The majority of acidic sites were located in Northern Europe, neutral sites in Middle Europe, and alkaline sites in Southern Europe (Table 3). These three geographical regions are shown in Figure 1, with borders at around 56 and 48°N. Most of the sampling sites in the Middle Europe region, that is, between these latitudes, had neutral pH. A fairly equal amount of Middle Europe sampling sites could be involved among the three pH classes (Table 3); however, they may not constitute a grouping by themselves but rather a transition zone between the Northern and Southern European regions.

Table 2

Fraction-Specific Median, Slope, and Intercept Values for Predictability of Elements (cf. Figure 3); Si/P/Ca/Mn: Fraction Specific Median Concentrations Represent Midpoint of the Data Point Distribution, and Numbers in Parentheses Represent the Percentage of, for Example, First Fraction Si as Sum Over All Samples Relative to All Particulate Si; Fe/Al/org C: Linear Regression Slope (m) and Intercepts (b) of \log_{10} Transformed Data. $n = 96$; unit: $\mu\text{mol/L}$, org C: mmol/L

	Si	P	Ca	Mn	Fe		Al		Org C	
	Median				m	b	m	b	m	b
First	0.03 (6.1)	0.04 (18.3)	0.67 (42.1)	0.001 (32.9)	1.00	−0.83	0.76	−0.55	1.71	−1.72
Second	0.02 (3.1)	0.12 (53.2)	1.32 (49.5)	0.003 (37.3)	0.85	−0.47	0.65	−0.57	0.88	−1.55
Third	0.08 (90.8)	0.08 (28.6)	0.24 (8.4)	0.002 (29.7)	0.72	−0.26	0.50	−0.07	0.56	−1.23
All part.	0.17	0.28	2.38	0.007						

Table 3
Number of Sampling Points in Each pH Class (Acidic pH <6.6, Neutral pH 6.6–7.3, and Alkaline pH >7.3) per GEOGRAPHIC Region (Figure 1)

	Acidic	Neutral	Alkaline	Total sampling points
North	24	7	0	31
Middle	5	10	8	23
South	8	2	32	42

Note. $n = 96$.

With some overlaps, the pH differences and the North-Middle-South groupings were reflected in the distribution patterns of elements among NNP and fine colloids (Figure 3). The elements with positive log-log relationships (e.g., Figure 3, top right and bottom right) exhibited some data point stratification, with lower elemental NNP and fine colloid concentrations at the Southern European and alkaline sites (red dots in Figure 3) and higher concentrations at the Northern European and acidic sites (green dots in Figure 3). Whether the main driver of this variation was really pH or a covariate related to pH warrants further attention (see also discussion below). The total concentrations of Ca, Si, Mn, and P increased from the Northern, acidic sites to the more alkaline streams in the South (Figure 3, top right and bottom left). Such behavior could well be expected for Ca but not necessarily for the other three elements (e.g., Song et al., 2002). The concentrations of Ca, Si, Mn, and P within NNP and fine colloid fractions did not vary systematically with total concentration but were roughly constant in their median value as the total concentrations increased from the Northern, acidic, sites to the more alkaline, Southern, sites. This implies that the elemental proportions that were bound to NNP and fine colloids decreased from North to South.

Eleven data points at three sites did not follow the clear regional stratification in the relationships between total and NNP/fine colloid concentrations (Figure 3); six Southern water samples for Ca (scattered relationship; two at SC and four at LZ) and five Northern water samples for Fe (all at AM; see Table 1 for site abbreviations). A concise explanation of their anomalous behavior could not be found, especially because the other elements did not exhibit this anomalous behavior, either in these samples or in any other samples. Site characteristics (Table 1) and stream water parameters at sampling (supporting information Table S1) showed no evident outliers in comparison to other sites within the same geographical region, with the exception of the three sites closest to the coast.

The presented data clearly showed the possibility to predict the concentrations of particle-bound elements, as some were independent of total concentrations (Ca, Si, Mn, and P) while others were linked (Fe, Al, and org C). Future research should address potential temporal patterns of NNP and fine colloid composition across an even larger, global scale.

3.4. Controlling Factors of NNP and Colloid Composition

The variable composition of NNP and fine colloids between sites and between sampling locations of one site can potentially be linked to differences in site parameters on larger (e.g., MAT or forest cover) or smaller (e.g., pH value or electrical conductivity) scale. As would be expected for large data sets, many statistically significant ($p < 0.05$) correlations for, for example, all particulate org C, Al, Ca, and Fe concentrations were found, but few strong correlations ($r > 0.71$) were found with site parameters (supporting information Table S3). Total Ca concentrations were tightly correlated with electrical conductivity ($r = 0.96$), which is unsurprising because Ca is often a significant fraction of total ionic strength, while all particulate Ca showed strong correlations to all particulate org C ($r = 0.84$) followed by catchment size ($r = 0.81$). In contrast, correlations between all particulate Si, P, Ca, and Mn and their total concentrations were weak ($r < 0.02$; partially negative values), as were the correlations between total element concentrations of, for example, Si and Mn and concentrations of other elements or site parameters ($r < 0.49$). However, concentrations of all particulate Si were positively related to concentrations of all particulate Al ($r = 0.72$) and especially strongly ($r = 0.98$) for Si and Al in the third size fraction, reflecting the presence of both elements in layer silicates such as clay minerals.

When particulate concentrations were correlated with site parameters, these correlations were rarely consistent among all size fractions. Marked differences were observed, for instance, between correlations of site parameters with the first and second fractions versus third fractions for Al and Si (supporting information Table S4). The correlations thus showed that relationships between site parameters and NNP and fine colloid concentrations differed, depending on the fraction in question, and that NNP and fine colloid concentrations cannot be explained through linear relationships alone.

At a KMO criterion >0.6 , we did not observe significant alterations in factor loadings with random elimination of data, and PCA was run stably with all particulate elemental concentrations, pH, MAT, conductivity, water temperature, and elevation, for instance. The PCA extracted four factors with eigenvalues >1 that jointly

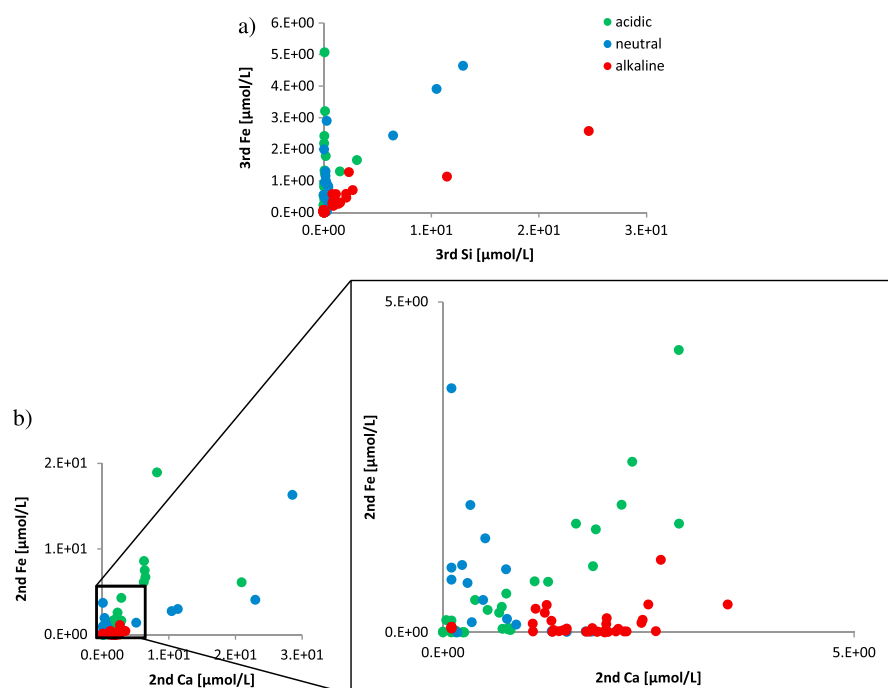


Figure 4. Example data plots of (a) third fraction Fe over third fraction Si and (b) second fraction Fe over second fraction Ca with zoom window. Color coding according to site pH class, acidic pH = green dots (pH < 6.6), neutral pH = blue dots (pH 6.6–7.3), and alkaline pH = red dots (pH > 7.3). $n = 96$.

explained 75% of the total variance. The resulting factor loadings revealed four distinct groupings of variables: (1) site parameters such as pH, water temperature, and MAT; (2) particulate Al and Si; (3) particulate org C, Ca, and Fe; and (4) particulate P (see supporting information Table S5).

Mattsson et al. (2009) showed a link between DOC and climatic and topographic factors through the strong positive correlation between DOC and latitude; here, however, the colloidal org C was rather related to that of Ca and Fe; this grouping even remained stable when including other site parameters into PCA at worse KMO test results. Fe (and Ca) are known to be key elements in reacting with soil C during microaggregation processes (see, e.g., Kögel-Knabner & Amelung, 2014), that is, our data would be in line with particles being released from riparian soils during riverbank erosion. Besides, our data showed that the NNP and fine colloid concentrations of Al and Si loaded highest at onto factor 2, thus supporting the results from above mentioned correlation analyses (supporting information Table S3) and indicating that clay minerals are always present within the third fine colloid fraction. Finally, the PCA analyses revealed that one factor can solely be assigned to particulate P. This is congruent with the simple correlation analyses and confirms that P cannot be predicted by simple linear statistical approaches across different geographic regions (see section 3.2). Overall, the factor loadings thus confirmed that different processes controlled the fate of different elements, while there was apparently no simple linear relation to site factors. Hence, we elucidated the contribution of soil, geology, vegetation, and pH class as additional controls of NNP and FC properties.

The pH value is often a master variable controlling chemical forms in solution (Perry et al., 2008) and may also determine the size and elemental composition of NNP and fine colloids (Neubauer et al., 2013). pH-dependent element abundances in a dissolved state are well understood in the context of nutrient availability (Perry et al., 2008) but not yet with respect to NNP and fine colloids. The geographic zoning of the streams more or less coincided with three dominant stream water pH classes (Figure 1 and Table 3). As shown for the third size fraction in Figure 4a, though also valid for all particulate Si (supporting information Figure S1), plotting Fe against Si clearly separated the acidic (Northern) streams from the alkaline (Southern) ones. Similar results were also obtained when, for example, plotting particulate Fe against particulate Ca as an indicator of calcareous bedrock (Figure 4b; illustrated for the second fraction; valid also for the first fraction but not for the third one; supporting information Figure S1). The findings can be reconciled with a study on Fe in

Table 4

Mean Values of All Particulate Molar Elemental Concentrations (mmol/L for org C, $\mu\text{mol/L}$ for Al, Si, P, Ca, and Mn) Across Classes Representing Groupings of Site Characteristics

		Org C	Al	Si	P	Ca	Mn	Fe	Number of sampling points
Soil class	Dystrophic	0.44 a	0.59 a	0.36 a	0.32 a	6.14 a	0.03 a	3.72 a	45
	Eutrophic	0.03 b	0.04 b	1.12 b	0.21 a	1.80 a	0.03 b	0.54 b	34
	Semiterrestrial	0.08 ab	0.05 ab	4.14 c	0.39 b	3.80 b	0.01 ab	1.04 ab	12
Bedrock class	Siliceous	0.37 a	1.77 a	0.35 a	0.32 a	5.50 a	0.03 a	3.12 a	54
	Calcareous	0.03 b	0.15 b	0.08 b	0.24 a	2.06 ab	0.04 a	0.09 b	22
	Flysch	0.08 b	3.36 c	4.96 c	0.30 a	3.89 b	0.01 a	1.24 a	10
Dominant forest type	Coniferous	0.47 a	2.50 a	1.13 a	0.30 a	6.64 a	0.031 a	5.11 a	54
	Broadleaf	0.03 b	1.02 b	1.16 b	0.20 b	1.77 b	0.028 b	0.56 b	26
pH class	Acidic	0.59 a	2.46 a	0.25 a	0.24 a	5.65 a	0.03 a	6.79 a	31
	Neutral	0.39 a	1.71 ab	0.47 a	0.39 a	7.89 a	0.03 a	3.47 ab	24
	Alkaline	0.04 b	1.62 b	2.11 a	0.29 a	2.47 a	0.03 a	0.76 b	41

Note. Significantly different classes per category and per element are marked by a, b and c; $p < 0.05$.

boreal catchments across different pH values (Neubauer et al., 2013). Fe entering stream waters is instantly oxidized and forms Fe(oxy)hydroxides or complexes with organic matter (Ekstrom et al., 2016), while formation of Ca- or Si-rich particles is likely independent from such processes. Overall, and despite the many complex factors regulating specific element concentrations in NNP and larger colloids, there are thus strong indicators of a geographic (or pH dependent) zoning of the composition of these particles. Forest biomass and soils, for instance, covary along our geographic transects, potentially affecting the pools and formation of humus and secondary minerals. Relevant factors could also be any covariates that induce nonlinear variations in element speciation across the pH range of 4.2 to 9.5 (Figure 4 and supporting information Table S1).

3.5. Impact of Specific Soil Types and Land Use on Element Concentrations

When grouping the sites, for example, according to soils, bedrock, and dominant forest type, at least one particulate elemental concentration was affected (Table 4), and the effects found for total particulate elemental concentrations were largely reflected in the individual size fractions as well (supporting information Tables S6–S8).

Sites characterized by semiterrestrial soils with better hydraulic connectivity to the streams showed significantly higher concentrations of colloidal Si than their counterparts with terrestrial soils (Kruskal-Wallis ANOVA; $p < 0.05$; Table 4). However, the more frequent redox cycles at the semiterrestrial sites (Blume et al., 2009) did not correlate with higher concentrations of redox-sensitive elements, at least as this particular sampling time. Since semiterrestrial soils are usually poor in soil structure (Blume et al., 2009), higher particulate Si concentrations in the streams could be related to riverbank erosion, but more data at higher temporal resolution would be needed to investigate this hypothesis.

Stream composition frequently correlates to the dominant bedrock (Krám et al., 2012). For the elements with positive log-log relationships (org C, Al, Fe; Figure 3, top right and bottom right), a significant differentiation between siliceous and calcareous rocks was found. The concentrations of org C, Al, Si, and Fe were higher for the siliceous sites (Table 4). Overall, it appeared that element release from siliceous sites was facilitated relative to the calcareous counterparts, which was accompanied by the release of these elements in all fractions of NNP and fine colloids (supporting information Table S6–S8). Particularly, high concentrations of Al and Si were found in the streams with flysch (Table 4), likely reflecting riverbank erosion of clay minerals (third colloidal fraction; supporting information Table S8) from the Gleysols in vicinity of the rivers. Note, however, that among our sites, bedrock classification yielded substantially more data points for siliceous than for calcareous rocks and flysch.

When the data were grouped according to the dominant forest type, the coniferous class differed significantly from the broadleaf class for all particulate org C, Al, P, Ca, and Fe concentrations, even for those of Si and Mn (Table 4; the one mixed stand was not included in this analysis). Notably, the element concentrations were generally larger in the coniferous tree stands than the broadleaved ones, consistent with the

tendency for coniferous stands to have more acidic stream waters (Allaby, 2006) and usually siliceous bedrocks (Table 1). In fact, almost 90% of the acidic sites were associated with dominant coniferous forest types (cf. Table 1 and supporting information Table S1). These conditions might generally favor NNP and fine colloid formation because low pH increases the density of positive charges of metal oxides and organic matter, which can then bind to negatively charged surfaces such as fine clay minerals as also outlined before (see also Tombácz et al., 2004). Indeed, when grouping our sites according to main pH classes as outlined above, the concentrations of particulate org. C, Al, and Fe were generally larger for the acidic sites (in Northern Europe) than for the alkaline ones (in Southern Europe). Interestingly, however, P did not exhibit this pH effect despite pH is the main variable affecting P availability and mobility in soils; hence, further analyses are necessary to help explain this effect.

4. Conclusions

Stream water sampling at 26 forested headwater catchments across Europe revealed substantial binding of Fe, P, Al, Mn, and org C to NNP and fine colloids. Overall, up to an average of $53 \pm 21\%$ of the total content of these elements in the stream waters occurred in three distinct particulate size fractions (first: < 20 nm, second: 20–60 nm, and third size fraction: >60 –300 nm). Particulate concentrations of org C, Fe, and Al increased with total concentrations of these elements from the south to the north, coincident with decreasing pH values and increasing portions of coniferous forests and siliceous bedrock. The sampled sites could be divided into sites that were characterized by the presence of Ca-containing NNP and fine colloids in alkaline stream waters and sites with an increasing predominance of Fe-NNP and fine colloids (acidic stream waters) because the Fe concentration superimposed Ca. This distinction was found for the first and second NNP fractions, whereas third size fraction (larger NNP and fine colloids) mainly consisted of Al- and Si-bearing clay minerals at all sites.

Interestingly, substantial amounts of P, which previously had been assigned to the operationally defined dissolved phase, were found to be associated with NNP and fine colloids. While P was mainly bound to Fe-containing particles of the first size fraction in more acidic Northern European headwaters, it was associated with Ca-bearing particles of the second size fraction in Southern European headwaters. Also, variations of total P were not correlated straightforwardly with variations of site characteristics across our sampling sites. Further efforts will be needed to better understand the complex interplay between total and colloidal P fluxes across the globe.

References

- Allaby, M. (2006). *Biomes of the Earth: Temperate forests*. New York: Chelsea House.
- Baken, S., Moens, C., van der Grift, B., & Smolders, E. (2016). Phosphate binding by natural iron-rich colloids in streams. *Water Research*, 98, 326–333. <https://doi.org/10.1016/j.watres.2016.04.032>
- Baken, S., Regelink, I. C., Comans, R. N., Smolders, E., & Koopmans, G. F. (2016). Iron-rich colloids as carriers of phosphorus in streams: A field-flow fractionation study. *Water Research*, 99, 83–90. <https://doi.org/10.1016/j.watres.2016.04.060>
- Benedetti, M. F., Van Riemsdijk, W. H., Koopal, L. K., Kinniburgh, D. G., Gooddy, D. C., & Milne, C. J. (1996). Metal ion binding by natural organic matter: From the model to the field. *Geochimica et Cosmochimica Acta*, 60(14), 2503–2513. [https://doi.org/10.1016/0016-7037\(96\)00113-5](https://doi.org/10.1016/0016-7037(96)00113-5)
- Binkley, D., Ice, G. G., Kaye, J., & Williams, C. A. (2004). Nitrogen and phosphorus concentrations in forest streams of the United States. *Journal of the American Water Resources Association*, 40(5), 1277–1291. <https://doi.org/10.1111/j.1752-1688.2004.tb01586.x>
- Bishop, K., Buffam, I., Erlandsson, M., Fölster, J., Laudon, H., Seibert, J., & Temnerud, J. (2008). Aqua incognita: The unknown headwaters. *Hydrological Processes*, 22(8), 1239–1242. <https://doi.org/10.1002/hyp.7049>
- Blume, H.-P., Brümmer, G. W., Horn, R., Kandeler, E., Kögel-Knabner, I., Kretzschmar, R., ... Wilke, B.-M. (2009). *Scheffer Schachtschabel: Lehrbuch Der Bodenkunde*. Berlin: Springer.
- Bol, R., Julich, D., Brödlin, D., Siemens, J., Kaiser, K., Dippold, M. A., ... von Blanckenburg, F. (2016). Dissolved and colloidal phosphorus fluxes in forest ecosystems—An almost blind spot in ecosystem research. *Journal of Plant Nutrition and Soil Science*, 179(4), 425–438. <https://doi.org/10.1002/jpln.201600079>
- Buffle, J., & Leppard, G. G. (1995). Characterization of aquatic colloids and macromolecules. 2. Key role of physical structures on analytical results. *Environmental Science & Technology*, 29(9), 2176–2184. <https://doi.org/10.1021/es00009a005>
- Celi, L., & Barberis, E. (2005). Abiotic stabilization of organic phosphorus in the environment. In B. Turner, E. Frossard, & D. Baldwin (Eds.), *Organic phosphorus in the environment* (pp. 113–132). Oxfordshire: CAB.
- Dahlqvist, R., Benedetti, M. F., Andersson, K., Turner, D., Larsson, T., Stolpe, B., & Ingri, J. (2004). Association of Calcium with colloidal particles and speciation of calcium in the Kalix and Amazon Rivers. *Geochimica et Cosmochimica Acta*, 68(20), 4059–4075. <https://doi.org/10.1016/j.gca.2004.04.007>
- Darch, T., Blackwell, M. S. A., Hawkins, J. M. B., Haygarth, P. M., & Chadwick, D. (2014). A meta-analysis of organic and inorganic phosphorus in organic fertilizers, soils, and water: Implications for water quality. *Critical Reviews in Environmental Science and Technology*, 44(19), 2172–2202. <https://doi.org/10.1080/10643389.2013.790752>

Acknowledgments

The authors gratefully acknowledge the assistance of the following people in locating suitable sampling sites, contacting site operators, performing the sampling, and providing data: A. Avila Castells (Autonomous University of Barcelona), R. Batalla (University of Lleida), P. Blomkvist (Swedish University of Agricultural Sciences), H. Bogena (Jülich Research Center), A.K. Boulet (University of Aveiro), D. Estany (University of Lleida), F. Garnier (French National Institute of Agricultural Research), H.J. Hendricks-Franssen (Research Center Jülich), L. Jackson-Blake (James Hutton Institute, NIVA), T. Laurila (Finnish Meteorological Institute), A. Lindroth (Lund University), M.M. Monerris (Universitat Politècnica de València), M. Ottosson Löfvenius (Swedish University of Agricultural Sciences), I. Taberman (Swedish University of Agricultural Sciences), F. Wendland (Research Center Jülich), F. Zetterberg (Swedish University of Agricultural Sciences and The Swedish Environmental Research Institute, IVL) and further unnamed contributors. The Swedish Infrastructure for Ecosystem Science (SITES) and the Swedish Integrated Monitoring, the latter financed by the Swedish Environmental Protection Agency, and ICOS Sweden have supported sampling and provided data for the Swedish sites. J. J. K. gratefully acknowledges the support from CESAM (UID/AMB/50017/ 2013), funded by the FCT/MCTES (PIDDAC) with cofunding by FEDER through COMPETE. N. G. gratefully acknowledges all those who contributed to organizing and implementing the continental sampling. The raw data can be found at <http://hdl.handle.net/2128/14937>. This project was partly funded by the German Research Foundation (DFG KL 2495/1-1).

- Dynesius, M., & Nilsson, C. (1994). Fragmentation and flow regulation of river systems in the northern 3rd of the world. *Science*, 266(5186), 753–762. <https://doi.org/10.1126/science.266.5186.753>
- Ektstrom, S. M., Regnell, O., Reader, H. E., Nilsson, P. A., Lofgren, S., & Kritzberg, E. S. (2016). Increasing concentrations of iron in surface waters as a consequence of reducing conditions in the catchment area. *Journal of Geophysical Research: Biogeosciences*, 121, 479–493. <https://doi.org/10.1002/2015JG003141>
- Erickson, H. P. (2009). Size and shape of protein molecules at the nanometer level determined by sedimentation, gel filtration, and electron microscopy. *Biological Proced Online*, 11(1), 32–51. <https://doi.org/10.1007/s12575-009-9008-x>
- Espinosa, M., Turner, B. L., & Haygarth, P. M. (1999). Preconcentration and separation of trace phosphorus compounds in soil leachate. *Journal of Environmental Quality*, 28(5), 1497–1504. <https://doi.org/10.2134/jeq1999.00472425002800050015x>
- Fernández-Martínez, M., Vicca, S., Janssens, I. A., Sardans, J., Luysaert, S., Campioli, M., ... Peñuelas, J. (2014). Nutrient availability as the key regulator of global forest carbon balance. *Nature Climate Change*, 4(6), 471–476. <https://doi.org/10.1038/nclimate2177>
- Giddings, J., Yang, F., & Myers, M. (1976). Flow-field-flow fractionation: A versatile new separation method. *Science*, 193(4259), 1244–1245. <https://doi.org/10.1126/science.959835>
- Gimbert, L. J., Andrew, K. N., Haygarth, P. M., & Worsfold, P. J. (2003). Environmental applications of flow field-flow fractionation (FIFFF). *Trac-Trends Analytical Chemistry*, 22(9), 615–633. [https://doi.org/10.1016/s0165-9936\(03\)01103-8](https://doi.org/10.1016/s0165-9936(03)01103-8)
- Gottselig, N., Bol, R., Nischwitz, V., Vereecken, H., Amelung, W., & Klumpp, E. (2014). Distribution of phosphorus-containing fine colloids and nanoparticles in stream water of a Forest catchment. *Vadose Zone Journal*, 13(7), 1–11. <https://doi.org/10.2136/vzj2014.01.0005>
- Gottselig, N., Nischwitz, V., Meyn, T., Amelung, W., Bol, R., Halle, C., ... Klumpp, E. (2017). Phosphorus binding to nanoparticles and colloids in Forest stream waters. *Vadose Zone Journal*, 16(3), 1–12. <https://doi.org/10.2136/vzj2016.07.0064>
- Hagedorn, A. G. (2006). EG-Sicherheitsdatenblatt (Gemäß 2001/58/EG), Nitrocellulose Rep.
- Hart, B. T., Douglas, G. B., Beckett, R., Vanput, A., & Vangrieken, R. E. (1993). Characterization of colloidal and particulate matter transported by the Magela Creek System, Northern Australia. *Hydrological Processes*, 7(1), 105–118. <https://doi.org/10.1002/hyp.3360070111>
- Hartland, A., Lead, J. R., Slaveykova, V., O'Carroll, D., & Valsami-Jones, E. (2013). The environmental significance of natural nanoparticles. *Nature Education Knowledge*, 4(8).
- Hasseloev, M., Lyven, B., Haraldsson, C., & Sirinawin, W. (1999). Determination of continuous size and trace element distribution of colloidal material in natural water by on-line coupling of flow field-flow fractionation with ICPMS. *Analytical Chemistry*, 71(16), 3497–3502. <https://doi.org/10.1021/ac981455y>
- Hasseloev, M., & von der Kammer, F. (2008). Iron oxides as geochemical nanovectors for metal transport in soil-river systems. *Elements*, 4(6), 401–406. <https://doi.org/10.2113/gselements.4.6.401>
- Hens, M., & Merckx, R. (2001). Functional characterization of colloidal phosphorus species in the soil solution of Sandy soils. *Environmental Science & Technology*, 35(3), 493–500. <https://doi.org/10.1021/es0013576>
- Hill, D. M., & Aplin, A. C. (2001). Role of colloids and fine particles in the transport of metals in rivers draining carbonate and silicate terrains. *Limnology and Oceanography*, 46(2), 331–344. <https://doi.org/10.4319/lo.2001.46.2.0331>
- Jarvis, H. P., Neal, C., Rowland, A. P., Neal, M., Morris, P. N., Lead, J. R., ... Hockenhull, K. (2012). Role of riverine colloids in macronutrient and metal partitioning and transport, along an upland-lowland land-use continuum, under low-flow conditions. *Science of the Total Environment*, 434, 171–185. <https://doi.org/10.1016/j.scitotenv.2011.11.061>
- Jiang, X.-Q., Bol, R., Nischwitz, V., Siebers, N., Willbold, S., Vereecken, H., Amelung, W., & Klumpp, E. (2015). Phosphorus Containing Water Dispersible Nanoparticles in Arable Soil. *Journal of Environmental Quality*, 44, 1772–1778. <https://doi.org/10.2134/jeq2015.02.0085>
- Kögel-Knabner, I., & Amelung, W. (2014). Dynamics, chemistry, and preservation of organic matter in soils. In H. D. Holland, & K. K. Turekian (Eds.), *Treatise on geochemistry*, (2nd ed.) (pp. 157–215). Oxford: Elsevier. <https://doi.org/10.1016/B978-0-08-095975-7.01012-3>
- Krámp, P., Hruška, J., & Shanley, J. B. (2012). Streamwater Chemistry in Three Contrasting Monolithologic Czech Catchments, *Applied Geochemistry*, 27, 1854–1863. <https://doi.org/10.1016/j.apgeochem.2012.02.020>
- Lyven, B., Hasseloev, M., Turner, D. R., Haraldsson, C., & Andersson, K. (2003). Competition between iron- and carbon-based colloidal carriers for trace metals in a freshwater assessed using flow field-flow fractionation coupled to ICPMS. *Geochimica et Cosmochimica Acta*, 67(20), 3791–3802. [https://doi.org/10.1016/s0016-7037\(03\)00087-5](https://doi.org/10.1016/s0016-7037(03)00087-5)
- Marschner, B., & Kalbitz, K. (2003). Controls of bioavailability and biodegradability of dissolved organic matter in soils. *Geoderma*, 113(3–4), 211–235. [https://doi.org/10.1016/s0016-7061\(02\)00362-2](https://doi.org/10.1016/s0016-7061(02)00362-2)
- Martin, J. M., Dai, M. H., & Cauwet, G. (1995). Significance of colloids in the biogeochemical cycling of organic-carbon and trace-metals in the Venice Lagoon (Italy). *Limnology and Oceanography*, 40(1), 119–131. <https://doi.org/10.4319/lo.1995.40.1.0119>
- Mattsson, T., Kortelainen, P., Laubel, A., Evans, D., Pujó-Pay, M., Räike, A., & Conan, P. (2009). Export of dissolved organic matter in relation to land use along a European climatic gradient. *Science of the Total Environment*, 407(6), 1967–1976. <https://doi.org/10.1016/j.scitotenv.2008.11.014>
- Missong, A., Bol, R., Willbold, S., Siemens, J., & Klumpp, E. (2016). Phosphorus forms in forest soil colloids as revealed by liquid-state ³¹P-NMR. *Journal of Plant Nutrition and Soil Science*, 179(2), 159–167. <https://doi.org/10.1002/jpln.201500119>
- Montalvo, D., Degryse, F., & McLaughlin, M. J. (2015). Natural colloidal P and its contribution to plant P uptake. *Environmental Science & Technology*, 49(6), 3427–3434. <https://doi.org/10.1021/es5046431>
- Neubauer, E., Köhler, S. J., von der Kammer, F., Laudon, H., & Hofmann, T. (2013). Effect of Ph and stream order on iron and arsenic speciation in boreal catchments. *Environmental Science & Technology*, 47(13), 7120–7128. <https://doi.org/10.1021/es401193j>
- Neubauer, E., vd Kammer, F., & Hofmann, T. (2011). Influence of carrier solution ionic strength and injected sample load on retention and recovery of natural nanoparticles using flow field-flow fractionation. *Journal of Chromatography, A*, 1218(38), 6763–6773. <https://doi.org/10.1016/j.chroma.2011.07.010>
- Nischwitz, V., & Goenaga-Infante, H. (2012). Improved sample preparation and quality control for the characterisation of titanium dioxide nanoparticles in sunscreens using flow field flow fractionation on-line with inductively coupled plasma mass spectrometry. *The Journal of Analytical Atomic Spectrometry*, 27(7), 1084–1092. <https://doi.org/10.1039/c2ja10387g>
- Perry, D. A., Oren, R., & Hart, S. C. (2008). 14.4 Chemical properties of soils. In *Forest ecosystems*, (pp. 269–281). Baltimore: JHU Press.
- Qafoku, N. P. (2010). Terrestrial nanoparticles and their controls on soil-geo-processes and reactions. In D. L. Sparks (Ed.), *Advances in agronomy*, (Vol. 107, pp. 33–91). San Diego, CA: Elsevier
- Ran, Y., Fu, J. M., Sheng, G. Y., Beckett, R., & Hart, B. T. (2000). Fractionation and composition of colloidal and suspended particulate materials in rivers. *Chemosphere*, 41(1–2), 33–43. [https://doi.org/10.1016/s0045-6535\(99\)00387-2](https://doi.org/10.1016/s0045-6535(99)00387-2)
- Ranville, J. F., & Macalady, D. L. (1997). Natural organic matter in catchments. In O. M. Saether, & P. De Caritat (Eds.), *Geochemical processes, weathering and groundwater recharge in catchments*, (pp. 263–303). Rotterdam: Balkema.

- Regelink, I. C., Koopmans, G. F., van der Salm, C., Weng, L., & van Riemsdijk, W. H. (2013). Characterization of colloidal phosphorus species in drainage waters from a clay soil using asymmetric flow field-flow fractionation. *Journal of Environmental Quality*, 42(2), 464–473. <https://doi.org/10.2134/jeq2012.0322>
- Regelink, I. C., Voegelin, A., Weng, L. P., Koopmans, G. F., & Comans, R. N. J. (2014). Characterization of colloidal Fe from soils using field-flow fractionation and Fe K-edge X-ray absorption spectroscopy. *Environmental Science & Technology*, 48(8), 4307–4316. <https://doi.org/10.1021/es405330x>
- Regelink, I. C., Weng, L., & van Riemsdijk, W. H. (2011). The contribution of organic and mineral colloidal nanoparticles to element transport in a Podzol soil. *Applied Geochemistry*, 26, S241–S244. <https://doi.org/10.1016/j.apgeochem.2011.03.114>
- Richardson, C. J. (1985). Mechanisms controlling phosphorus retention capacity in fresh-water wetlands. *Science*, 228(4706), 1424–1427. <https://doi.org/10.1126/science.228.4706.1424>
- Roth, C. (2011). Sicherheitsdatenblatt Gemäß Verordnung (EG) Nr. 1907/2006, Cellulose Für Die Säulenchromatographie Rep.
- Schmitt, D., Taylor, H. E., Aiken, G. R., Roth, D. A., & Frimmel, F. H. (2002). Influence of natural organic matter on the adsorption of metal ions onto clay minerals. *Environmental Science & Technology*, 36(13), 2932–2938. <https://doi.org/10.1021/es010271p>
- Sharpley, A., Hedley, M. J., Sibbesen, E., Hillbricht-Ilkowska, A., House, A., & Ryszkowski, L. (1995). Phosphorus transfers from terrestrial to aquatic eco-systems. In *Phosphorus in the global environment-transfers, cycles and management, scope 54*, (pp. 171–199). New York: John Wiley.
- Six, J., Elliott, E. T., & Paustian, K. (1999). Aggregate and soil organic matter dynamics under conventional and no-tillage systems. *Soil Science Society of America Journal*, 63(5), 1350–1358. <https://doi.org/10.2136/sssaj1999.6351350x>
- Song, Y., Hahn, H., & Hoffmann, E. (2002). Effects of pH and ca/P ratio on the precipitation of phosphate. In *Chemical water and wastewater treatment*, (Vol. VIII, pp. 349–362). London, UK: WA Publishing Alliance House.
- Stolpe, B., Guo, L., Shiller, A. M., & Hasselov, M. (2010). Size and composition of colloidal organic matter and trace elements in the Mississippi River, Pearl River and the northern Gulf of Mexico, as characterized by flow field-flow fractionation. *Marine Chemistry*, 118(3–4), 119–128. <https://doi.org/10.1016/j.marchem.2009.11.007>
- Stumm, W., & Morgan, J. J. (1981). *Aquatic chemistry: An introduction emphasizing chemical equilibria in natural waters*. New York: John Wiley.
- Tipping, E., & Hurley, M. (1992). A unifying model of cation binding by humic substances. *Geochimica et Cosmochimica Acta*, 56(10), 3627–3641. [https://doi.org/10.1016/0016-7037\(92\)90158-F](https://doi.org/10.1016/0016-7037(92)90158-F)
- Tombácz, E., Libor, Z., Illés, E., Majzik, A., & Klumpp, E. (2004). The Role of Reactive Surface Sites and Complexation by Humic Acids in the Interaction of Clay Mineral and Iron Oxide Particles. *Organic Geochemistry*, 35, 257–267. <http://doi.org/10.1016/j.orggeochem.2003.11.002>
- Trostle, K. D., Ray Runyon, J., Pohlmann, M. A., Redfield, S. E., Pelletier, J., McIntosh, J., & Chorover, J. (2016). Colloids and organic matter complexation control trace metal concentration-discharge relationships in Marshall gulch stream waters. *Water Resources Research*, 52(10), 7931–7944. <https://doi.org/10.1002/2016WR019072>
- U.S. Department of Agriculture (1993). Soil survey manual, chapter 3. Selected chemical properties.
- Vitousek, P. (1982). Nutrient cycling and nutrient use efficiency. *The American Naturalist*, 119(4), 553–572. <https://doi.org/10.1086/283931>
- Wells, M. L., & Goldberg, E. D. (1991). Occurrence of small colloids in sea water. *Nature*, 353(6342), 342–344. <https://doi.org/10.1038/353342a0>
- Wen, L. S., Santschi, P., Gill, G., & Paternostro, C. (1999). Estuarine trace metal distributions in Galveston Bay: Importance of colloidal forms in the speciation of the dissolved phase. *Marine Chemistry*, 63(3–4), 185–212. [https://doi.org/10.1016/s0304-4203\(98\)00062-0](https://doi.org/10.1016/s0304-4203(98)00062-0)
- Zirkler, D., Lang, F., & Kaupenjohann, M. (2012). “Lost in filtration”—The separation of soil colloids from larger particles. *Colloids and Surfaces, A: Physicochemical and Engineering Aspects*, 399, 35–40. <https://doi.org/10.1016/j.colsurfa.2012.02.021>